# GLOBALLY OPTIMAL GEOMETRIC SEGMENTATION OF FILAMENTS

*Xun Xiao[1] and Ivo F. Sbalzarini[1]*

## ABSTRACT

Filamentous structures are commonplace in biology. The thickness of biological filaments is often below the resolution limit of the microscope, and the SNR of images is often low, requiring robust model-based image-processing methods that account for the optical properties of the microscope and the biophysical properties of the imaged filaments. Our method represents filaments by parametric curves that are optimally segmented in two steps: solving a globally convex optimization for filament detection and evolving a local model for each filament by gradient descent.

## 1. METHOD

### 1.1. Global Filament Detection

We detect filament regions by globally optimizing the following energy functional over the segmentation (pixel mask) $\Omega$:

$$\mathcal{E}(\boldsymbol{\beta}, \Omega) = \int \mathbf{B}_{b^*}\Big(u(\boldsymbol{x}) \parallel u_\Omega(\boldsymbol{x})\Big)\mathrm{d}\boldsymbol{x} + \lambda \mathrm{TV}(\Omega). \quad (1)$$

The first term measures the Bregman divergence $\mathbf{B}_{b^*}$ between the observed image $u(\boldsymbol{x})$ and the expected one under a given segmentation $\Omega$. As a regularizer we use the popular total variation (TV) penalty. We use an alternating split-Bregman algorithm to globally minimize this convex energy [1].

### 1.2. Local Parametric Curve Evolution

We initialize one parametric B-spline curve $c_i(s)$ for each detected filament $i$. In each iteration of the gradient-descent procedure, we perturb the position of a control point $p_m^i$ of each spline $i$ by a value $\Delta_i$, resulting in the finite-difference approximation to the gradient:

$$\mathcal{G}'(p_m^i) = \frac{1}{\Delta_i}\mathcal{E}(c_i(p_m^i + \Delta_i)) - \mathcal{E}(c_i). \quad (2)$$

The spline nodes are then updated to $p_m^i \leftarrow p_m^i - \alpha p_m^i \mathcal{G}'(p_m^i)$ with step size $\alpha$. This procedure is repeated for all nodes $m$ until $|\mathcal{G}'| < \epsilon$ for some small tolerance $\epsilon$.

## 2. RESULTS

We benchmark our method using synthetic images. The $\ell_2$ and $\ell_\infty$ norms of the deviations of the segmented curve from the ground truth are shown in Fig. 1. We compare our method with SOAC [2] in Fig. 2a and demonstrate it on real fluorescence microscopy data in Fig. 2b.
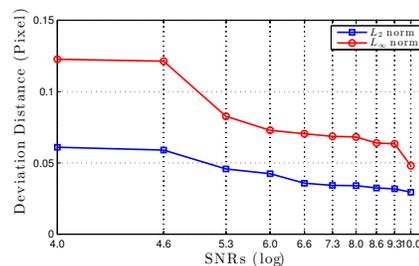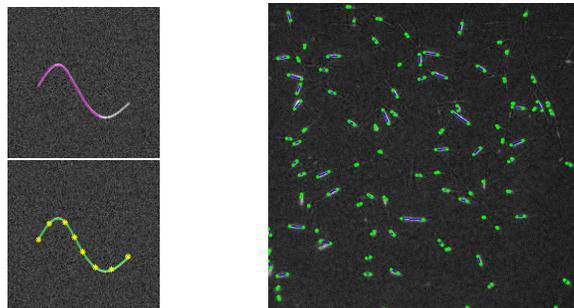


**Fig. 1**: Localization error vs. PSNR (log)



(a) SOAC [2] (top) and our method (bottom) for a synthetic image with PSNR=4.

(b) Confocal image of microtubules *in vitro* (image: Dr. Reber, Hyman lab, MPI-CBG)

**Fig. 2**: Comparison and application to real data.

## 3. REFERENCES

[1] G. Paul, J. Cardinale, and I. F. Sbalzarini, "Coupling image restoration and segmentation: A generalized linear model/Bregman perspective," *Intl. J. Comp. Vis.*, pp. 1–25, 2013.

[2] M. B. Smith, H. Li, T. Shen, X. Huang, E. Yusuf, and D. Vavylonis, "Segmentation and tracking of cytoskeletal filaments using open active contours," *Cytoskeleton*, vol. 67, no. 11, pp. 693–705, 2010.